ACS OMEGA

Open Access



http://pubs.acs.org/journal/acsodf

Article

# Targeted Screening of Curcumin Derivatives as Pancreatic Lipase Inhibitors Using Computer-Aided Drug Design

Yuxuan Jing,[#] Laichun Luo,[#] Zhaoxiang Zeng,[#] Xueyan Zhao, Rongzeng Huang, Chengwu Song, Guiying Chen, Sha Wei, Haijun Yang, Yinping Tang,* and Shuna Jin*

Cite This: *ACS Omega* 2024, 9, 27669−27679

Read Online

ACCESS | Metrics & More | Article Recommendations | Supporting Information

**ABSTRACT:** Curcumin has demonstrated promising preclinical antiobesity effects, but its low bioavailability makes it difficult to exert its full effect at a suitable dose. The objective of this study was to screen curcumin derivatives with enhanced bioavailability and lipid-lowering activity under the guidance of computer-aided drug design (CADD). CAAD was used to perform virtual assays on curcumin derivatives to assess their pharmacokinetic properties and effects on pancreatic lipase activity. Subsequently, 19 curcumin derivatives containing 5 skeletons were synthesized to confirm the above virtual assay. The in vitro pancreatic lipase inhibition assay was employed to determine the half-maximal inhibitory concentration ($IC_{50}$) of these 19 curcumin derivatives. Based on CADD analysis and in vitro pancreatic lipase inhibition, 2 curcumin derivatives outperformed curcumin in both aspects. Microscale thermophoresis (MST) experiments were employed to assess the binding equilibrium constants ($K_d$) of the aforementioned 2 curcumin derivatives, curcumin, and the positive control drug with pancreatic lipase. Through virtual screening utilizing a chemoinformatics database and molecular docking, 6 derivatives of curcumin demonstrated superior solubility, absorption, and pancreatic lipase inhibitory activity compared to curcumin. The $IC_{50}$ value for 1,7-bis(4-hydroxyphenyl)heptane-3,5-dione (C4), which displayed the most effective inhibitory effect, was 42.83 $\mu$M, while the $IC_{50}$ value for 1,7-bis(4-hydroxy-3-methoxyphenyl)heptane-3,5-dione (C6) was 98.62 $\mu$M. On the other hand, the $IC_{50}$ value for curcumin was 142.24 $\mu$M. The MST experiment results indicated that the $K_d$ values of C4, C6, and curcumin were 2.91, 18.20, and 23.53 $\mu$M, respectively. The results of the activity assays exhibited a relatively high degree of concordance with the outcomes yielded by CADD screening. Under the guidance of CADD, the targeted screening of curcumin derivatives with excellent properties in this study exhibited high-efficiency and low-cost benefits.

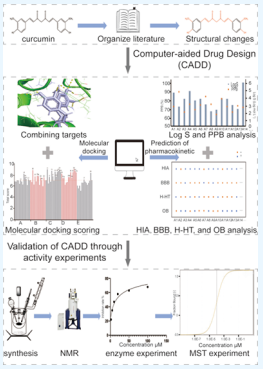


## 1. INTRODUCTION

Turmeric (*Curcuma longa* L.), the dried rhizome of the ginger plant, is widely used as a dual-purpose food and medicine.[1] It has been shown to have minimal inherent toxicity and exhibits various pharmacological activities, including anti-inflammatory, hypolipidemic, and hypoglycemic properties.[2,3] Obesity constitutes a ubiquitous global public health challenge, precipitating numerous deleterious health complications.[4] Curcumin is regarded as the principal bioactive component of turmeric, and it has been demonstrated to enhance the capacity to ameliorate obesity by reducing hepatic and plasma lipid levels.[5] However, the limited water solubility and poor absorption of curcumin impede its effective utilization and hinder further development.[6] Therefore, it is imperative to explore potential strategies that can enhance the efficacy of curcumin.

In order to enhance the lipid-lowering activity of curcumin by ameliorating its unfavorable characteristics, exploration has been conducted on various approaches, including nano-formulations of curcumin,[7] intestinal microbiota metabolism,[8] structural modifications,[9] and synergistic utilization with other drugs.[10] The aforementioned approaches exhibit promising potential in ameliorating the undesirable characteristics of curcumin. However, most of them often fail to avoid the substantial time and cost expenditures incurred during the preliminary investigation of curcumin.[11,12] Hence, expediting the acquisition of the desired target compound within a shorter development cycle is a pressing and imperative concern.

With the rapid advancement of artificial intelligence, computer-aided drug design (CADD) screening holds the potential to significantly reduce the substantial costs associated with conventional drug development.[13] It can predict, screen, and lead optimize compounds based on their structure or potential pharmacological groups.[14,15] Based on its primary focus on compound structures and the screening properties related to target receptors, CADD enables seamless alignment with the property alterations resulting from the structural

**Received:** April 14, 2024
**Revised:** May 30, 2024
**Accepted:** June 3, 2024
**Published:** June 13, 2024





https://doi.org/10.1021/acsomega.4c03596
*ACS Omega* 2024, 9, 27669−27679

modifications of curcumin.[16] The application of CADD enables high-throughput screening of various distinct characteristics arising from structural modifications of curcumin derivatives. This facilitates the rapid and effective acquisition of compounds demonstrating superior bioavailability and activity compared to curcumin. Subsequently, guided by the screening outcomes, targeted synthesis of derivatives can effectively mitigate the cost incurred by the blind synthesis. The accuracy and reliability of the screening results can be ensured through specific activity testing and evaluation. The activity assays encompass both traditional in vitro pancreatic lipase inhibition assays and innovative microscale thermophoresis (MST). MST is a technique that detects changes in the migration rate of biomolecules in a temperature gradient, enabling the exploration of binding and dissociation processes between biomolecules and acquisition of information regarding patterns of molecular interactions and kinetic constants.[17,18]

In this study, variations in the linear skeleton and substituent of curcumin derivatives were sorted through a literature search. CADD assessed the drug-likeness, aqueous solubility (LogS), human intestinal absorption (HIA), plasma protein binding (PPB), blood-brain barrier permeability (BBB), hepatotoxicity (H-HT), and oral bioavailability (OB) of curcumin derivatives. The effect of 19 curcumin derivatives on the inhibition of pancreatic lipase was developed with the help of molecular docking methods. To validate the results of CADD screening, we obtained standard samples of certain curcumin derivatives and further investigated their activities against pancreatic lipase through in vitro enzyme inhibition assays and MST. This experiment was the first instance of using CADD to evaluate the activity of curcumin derivatives against pancreatic lipase.

## 2. MATERIALS AND METHODS

**2.1. Chemicals and Reagents.** HPLC grade acetonitrile was purchased from Merck (Merck, New Jersey, USA). Deionized water was prepared using an ultrapure water system (Pgwater, Wuhan China). Deuterated reagents were obtained from Sigma-Aldrich (Sigma-Aldrich, St. Louis, USA). Pancreatic lipase (CAS: 9001-62-1), 4-nitrophenyl butyrate, and orlistat were purchased from Macklin Biochemical (Macklin, Shanghai, China). Tris and Tris−HCl were acquired from Solarbio Biotechnology (Solarbio, Beijing, China). The RED-NHS second-generation dye, NHS-labeled buffer, and protein sample purification column were all purchased from Nanotemper (Nanotemper, Munich, Germany). Human-derived pancreatic lipase, PBS buffer, and Tween 20 were acquired from Sigma-Aldrich (Sigma-Aldrich, St. Louis, USA). Raw materials were obtained from Energy Chemical (Energy, Anhui, China), including tributyl borate, diboron trioxide, *n*-butylamine, acetone, 3,4-dimethoxybenzaldehyde, 3,4,5-trimethoxybenzaldehyde, nickel chloride hexahydrate, p-hydroxybenzaldehyde, 3-hydroxy-4-methoxybenzaldehyde, and 3,4-dihydroxybenzaldehyde. Thin-layer chromatography (TLC) and silica gel column chromatography were purchased from Qingdao Ocean Chemical (QOC, Qingdao, China).

**2.2. Determination of Curcumin Derivatives.** The determination of the structural derivatives of curcumin was obtained through the compilation of relevant research literature. Alterations in the quantity of methoxy and hydroxy groups on the phenyl ring substituents of curcumin exhibited varying degrees of influence on its polarity, water solubility, and pharmacological efficacy.[19−21] Monocarbonyl curcumin, dihydrocurcumin, tetrahydrocurcumin, and octahydrocurcumin had been demonstrated to outperform curcumin in terms of stability, bioavailability, and activity.[22−24] Based on the aforementioned reasons, we had identified the substitution positions and quantities of methoxy and hydroxy groups on the phenyl ring of curcumin as well as structural modifications of double bonds and $\beta$-diketones on the backbone. Ultimately, curcumin derivatives were obtained through a linear arrangement for CADD analysis.

**2.3. Property Prediction of Curcumin Derivatives.** The analysis of drug-like properties, LogS, HIA, PPB, BBB, OB, and H-HT of curcumin derivatives was conducted on ADMETlab 2.0 (https://admetmesh.scbdd.com/).

In order to assess the potential of curcumin derivatives as therapeutic agents, the Lipinski rule was employed to assess whether a compound exhibited pharmacological properties.[25] This required a molecular weight (MW) of <500, a partition coefficient (LogP) of <5, fewer than 5 hydrogen bond donors (Hdon), fewer than 10 hydrogen bond acceptors (Hacc), and fewer than 10 rotatable bonds (RBN).[26] If any two or more of these rules were violated, oral absorption by living organisms became challenging.

Upon the completion of assessing the drug-like properties of curcumin derivatives, the subsequent evaluation pertained to the properties influencing their pharmacological efficacy in vivo. First, to appraise the aqueous solubility impacting the in vivo translocation, distribution, and transmembrane capability of curcumin derivatives, the LogS was predicted.[27] Second, to analyze the in vivo effectiveness of curcumin derivatives, predictions were made regarding HIA, BBB, PPB, H-HT, and OB.

**2.4. Molecular Docking and Dynamics Simulation.** SYBYL-X 2.0 (Trepos, New Jersey, USA) was employed for molecular docking, and Pymol (Schrödinger, New York, USA) was utilized for processing saved files, analyzing amino acid residues and binding conformations, and generating ligand interaction diagrams. Discovery Studio 2019 (Dassault Systèmes, Paris, France) was employed to conduct molecular dynamics simulations of curcumin derivatives with pancreatic lipase.

The 2D structure of orlistat was obtained from PubChem (https://www.ncbi.nlm.nih.gov/pccompound/3034010), while the structures of curcumin and its derivatives were constructed in ChemDraw. The sketch function was utilized for hydrogenation and conformational optimization. The PDB format of pancreatic lipase (PDB ID: 1LPB) was downloaded from RCSB PDB (http://www.rcsb.org/pdb/home/home.do). The molecular docking module Docking Suite was employed to optimize the enzyme protein, including the removal of crystal water, hydrogenation of charges, protein structure repair, and generation of docking pockets. The study employed the SFXC mode, a high-precision docking mode, for molecular docking. This mode was based on a search engine of molecular shape similarity, employing prototype molecules to delineate protein binding pockets. It utilized probes to detect surface hydrophobicity, hydrogen bonding, and electrostatic properties of the protein pocket, ultimately facilitating the docking of ligand molecules to the protein's binding site. Subsequently, enzyme-ligand files were generated and saved in the molecular SD format. During the assembly process, the total score (TS) was calculated and the results were analyzed. Following solvation of the protein, molecular dynamics simulations were conducted. The molecular dynamics simulation process entailed optimization, heating, equilibration, and sampling of


https://doi.org/10.1021/acsomega.4c03596
ACS Omega 2024, 9, 27669−27679

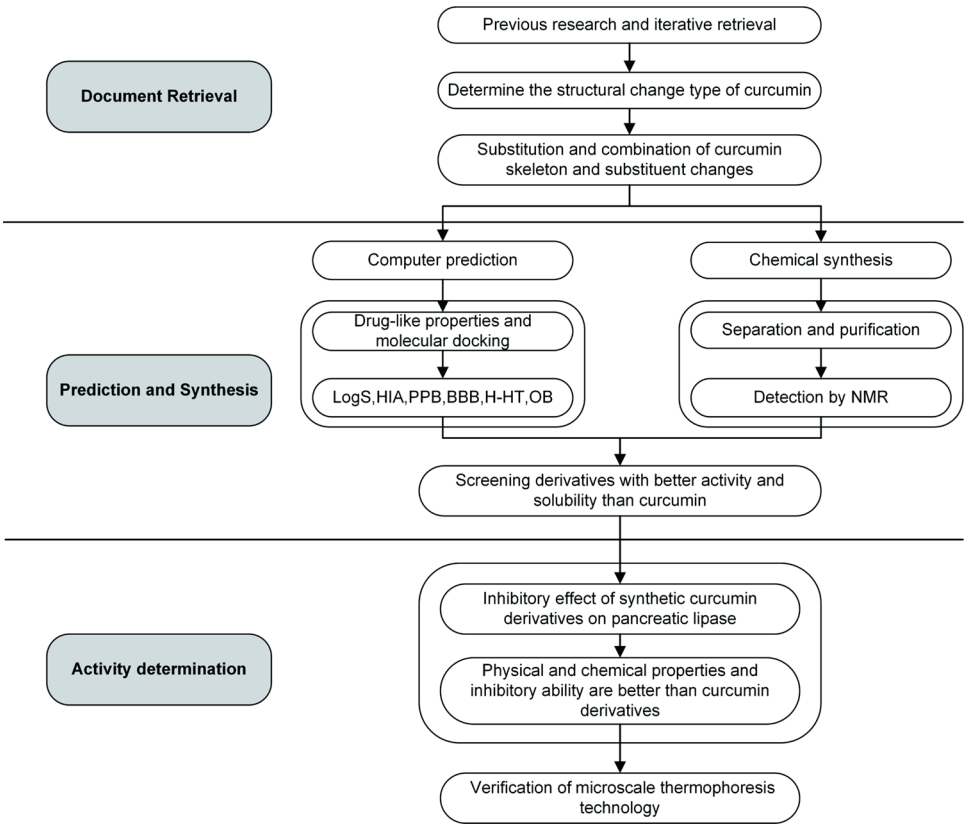


**Figure 1.** Integrating the analytical strategy of computer-aided drug design screening and in vitro experimental validation.

the protein-small molecule complex. The simulation results were utilized for trajectory analysis to obtain the root-mean-square deviation curves (RMSD) and root-mean-square fluctuation curves (RMSF).

**2.5. Synthesis of Curcumin Derivative Standards.** The synthetic steps for curcumin derivatives, encompassing a repertoire of 5 distinct frameworks, are delineated in Figure S1.[28,29] Thin-layer chromatography (TLC) was performed for component identification, and silica gel column chromatography was employed for separation and purification. The synthesis reaction in this experiment was based on the aldol condensation reaction between aldehyde groups and the hydrogenation and reduction reaction of carbon−carbon double bonds in a hydrogen environment with Pd/C catalysis. This route offered mild reaction conditions and a high yield. The synthesized compounds were subsequently well-characterized by using NMR. A 20 mg aliquot of curcumin derivative, intended for nuclear magnetic resonance analysis, was dissolved in 0.5 mL of the deuterated reagent. $^{1}$H NMR (400 M) and $^{13}$C NMR (101 M) spectra were recorded on Bruker Ascend 400 spectrometers (Bruker, Massachusetts, Switzerland).

**2.6. Pancreatic Lipase Inhibition Test of Curcumin Derivatives.** The pH was measured by using a PHS-2F pH meter (Inesa, Shanghai, China), and the enzyme marker used was the Tecan Infinite F50 enzyme marker (Tecan, Zurich, Switzerland).

The pancreatic lipase inhibition experiment followed a standardized protocol.[30,31] The reaction system comprised 80 $\mu$L of Tris−HCl buffer (50 mM, pH 7.5), 60 $\mu$L of enzyme solution (2.5 mg mL$^{-1}$), 40 $\mu$L of pancreatic lipase inhibitor (curcumin derivatives: 2, 5, 10, 20, 50, and 100 $\mu$g mL$^{-1}$; orlistat: 0.125, 0.25, 0.5, 1.0, 2.0, and 4.0 $\mu$g mL$^{-1}$), and 60 $\mu$L of 4-nitrophenyl butyrate substrate solution (2 mg mL$^{-1}$). It was ensured that the concentration of dimethyl sulfoxide (DMSO) in the solution system was less than 5%. The curve was fitted at 405 nm to calculate the change rate of the absorbance over time. The percent inhibition was calculated using the following formula:

$$\%\text{Inhibition} = [1 - K_a - K_b/K_c] \times 100\%$$

Here, $K_a$ represents the change rate of absorbance caused by enzyme reaction after addition of the inhibitor, $K_b$ is the change rate of absorbance caused by enzyme reaction without addition of the inhibitor, and $K_c$ is the change rate of absorbance caused by enzyme reaction without addition of the inhibitor.

**2.7. MST Experiment of Curcumin Derivatives.** The MST analysis of compounds and pancreatic lipase was conducted using Monolith NT.115 (Nanotemper, Munich, Germany). The affinity results were presented on the MO.Control and MO.Affinity Analysis platforms (Nanotemper, Munich, Germany).

The final dye solution, with a concentration of 300 $\mu$M, was prepared by combining 7 $\mu$L of the second-generation RED-NHS dye solution (600 $\mu$M, dissolved in DMSO) with 7 $\mu$L of the labeled buffering agent NHS (dissolved in 3 mL of distilled water). The dye-protein solution, a total of 100 $\mu$L, consisted of 90 $\mu$L of trypsin solution (10 $\mu$M, dissolved in PBST) and 10 $\mu$L of the final dye solution. The dye-protein solution was then incubated in darkness at room temperature for 30 min. Subsequently, the purified labeled protein solution was obtained through protein purification by column filtration. Subsequently, the affinity between curcumin derivatives and


https://doi.org/10.1021/acsomega.4c03596
ACS Omega 2024, 9, 27669−27679

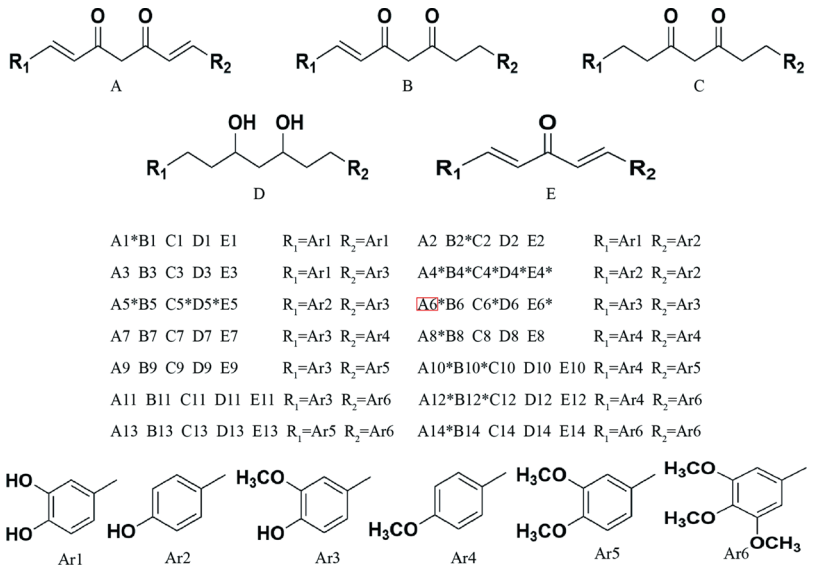


**Figure 2.** Structures of curcumin derivatives were determined through literature retrieval. They were classified by different skeletons (A−E) and substituents (1−14) on different benzene rings. Synthetic compounds are marked with * in the upper right corner of their respective ID numbers. The red border indicates curcumin.

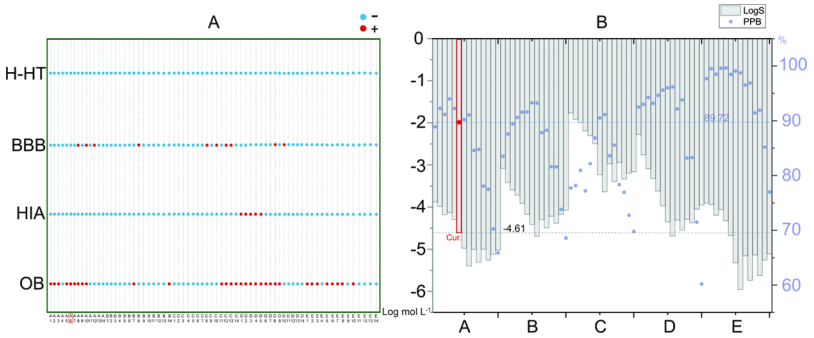


**Figure 3.** Performing an analysis of the properties of curcumin derivatives utilizing a pharmaceutical physicochemical property database facilitated by computer technology. (A) Analysis of OB, BBB, HIA and H-HT, blue is negative, and red is positive. (B) Analysis of PPB and LogS, among them, the blue dotted line is the value of PPB of curcumin, which was 89.72%, and the gray dotted line is the value of curcumin LogS, which was −4.61 Log mol $L^{-1}$. The red border and mark indicate curcumin; "Cur." is its abbreviation.

pancreatic lipase was analyzed at a reaction temperature of 37 °C.

**2.8. Strategy Analysis of CADD.** As shown in Figure 1, this study used a method combined with the CADD experience. Initially, we determined the types of structural changes in curcumin derivatives through a review of relevant literature and our previous reports.[32,33] After the substituents and skeletal modifications of the curcumin derivatives were determined, the structures of these derivatives were linearly arranged to generate a cohort of curcumin derivatives for subsequent analysis. We conducted evaluations of the curcumin derivatives in terms of their drug-likeness, LogS, HIA, PPB, BBB, H-HT, and OB. Through this screening process, we identified derivatives that surpassed curcumin in terms of all of these aspects. To ensure that the curcumin derivatives possess improved pharmacokinetic properties along with superior pancreatic lipase inhibitory activity, their interaction with pancreatic lipase was assessed using a molecular docking evaluation. By integrating the aforementioned evaluations, we screened curcumin derivatives that exhibited enhanced bioavailability and pancreatic lipase inhibition activity. In order to ensure the reliability of the experimental results, we utilized chemical synthesis to obtain a set of standardized curcumin derivatives after conducting CADD evaluations. Subsequently, we conducted separate in vitro pancreatic lipase inhibition experiments and MST assays to evaluate the inhibitory potency and binding affinity of the curcumin derivatives toward pancreatic lipase.

**2.9. Data Analysis.** Graphs and statistical analyses were constructed by using GraphPad Prism 7 (GraphPad Software, California, US). Tables and figures were constructed using Adobe Illustrator 2022 (Adobe, California, US). HRMS analysis was conducted using Mestrenova 14.0.0 (Mestrelab Research, Galicia Autonomous Region, Spain).

## 3. RESULTS

**3.1. Screening of Curcumin Derivatives with CADD.** As shown in Figure 2, a total of 70 predicted derivatives of curcumin were identified with their names listed in Table S1. These derivatives were composed of a linear arrangement of 5 structural frameworks and 14 substituents. The five structural frameworks were denoted by the letters A, B, C, D, and E, respectively. Within each structural framework, there were 14 derivative compounds formed based on the arrangement of


https://doi.org/10.1021/acsomega.4c03596
ACS Omega 2024, 9, 27669−27679

substituents, and A6 represented curcumin. The evaluation results of drug-like properties are shown in Table S2. All compounds met the specified criteria, with none of the parameters exceeding the predetermined range simultaneously. All curcumin derivatives had the potential to be developed into drugs. The pharmacokinetic analysis of curcumin derivatives is illustrated in Figure 3 and Table S3. In Figure 3A, the results for H-HT, BBB, HIA, and OB of curcumin are depicted in both negative and positive aspects, where curcumin derivatives displaying negativity across all four metrics exhibited properties superior to curcumin. In Figure 3B, LogS and PPB of curcumin are numerically represented, with curcumin derivatives demonstrating values, where LogS exceeded that of curcumin and PPB was lower than curcumin, showcasing properties superior to curcumin. The water solubility analysis indicated that 50 curcumin derivatives exhibited higher water solubility compared to curcumin. PPB analysis revealed that 33 curcumin derivatives had a lower PPB than curcumin. Besides, using a 30% OB threshold for prediction, 38 curcumin derivatives demonstrated OB values higher than those of curcumin. With the exception of D1, D2, D3, D4, and D5, whose absorption rates were all below 30%, all other curcumin derivatives exhibited good HIA. Apart from A8, A10, A12, B8, B10, C8, C10, C12, C13, D8, and D10, all other curcumin derivatives demonstrated low BBB permeability. All compounds exhibited a propensity for the absence of H-HT.

The molecular docking results are presented in Figure 4 and Table S4. The TS of curcumin was 7.0624. The molecular

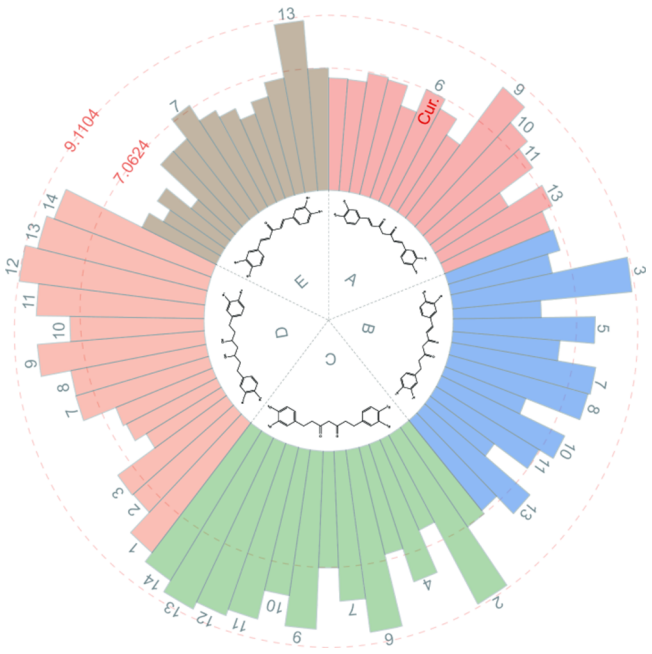


**Figure 4.** Molecular docking of curcumin derivatives with pancreatic lipase. The dotted line in the inner circle is 7.0624 for curcumin docking, and the dotted line in the outer circle is the maximum docking score, that is, 9.1104 for D12 and pancreatic lipase. "Cur." is the abbreviation for curcumin.

docking screening of curcumin derivatives indicated that 35 of them exhibited a stronger pancreatic lipase binding capacity than curcumin. Thus, in summarizing the analysis results aided by CADD, it was found that B3, C2, C4, C6, C9, and D14 exhibited superior physical and chemical properties compared with curcumin in all evaluation parameters. As depicted in Figure 5 and Table S5, the interaction targets of 6 curcumin derivatives, which were identified through CADD screening, with pancreatic lipase are elucidated. The ligand interaction diagram is depicted in Figure S2. The amino acid sites involved in binding of orlistat to pancreatic lipase were SER-152, LEU-153, HIS-151, PHE-77, and GLY-76. The primary binding amino acids for pancreatic lipase and curcumin derivatives were SER-152, HIS-151, PHE-77, and ARG-256. The molecular dynamics simulation results of curcumin derivatives C2, C4, C6, C9, B3, and D12, along with curcumin and orlistat, are presented in Figure S3. The RMSD for C4, C6, curcumin, and orlistat fell within the range of 0.75−3.0 Å, while their RMSF values remained below 3.0 Å. The RMSD ranges for C2 and C9 were similar, falling within the range of 0.8−5.0 Å, while their RMSF values lay within the range of 0.5−4.5 Å. The overall RMSF values for D14 and B3 remained stable; however, their RMSD exhibited the largest fluctuations, ranging between 1.0 and 8.0 Å

**3.2. Synthesis of Curcumin Derivative Standards.** After the use of CADD to screen the physicochemical properties of curcumin derivatives, it was imperative to proceed with obtaining specific experimental data for these compounds. Employing methods of chemical synthesis became instrumental in acquiring a collection of curcumin derivatives, showcasing diverse performances as predicted. As shown in Figure 2, the asterisk (*) in the upper right corner indicates the synthesized derivatives of curcumin. Nineteen derivatives of curcumin, including curcumin itself, had been synthesized. The selection of these curcumin derivatives for synthesis was a comprehensive consideration of the requirements of the structural framework, the screening outcomes of CADD, and the feasibility of synthesis. The detailed synthetic methods of 19 curcumin derivatives are illustrated in Scheme S1. The NMR data and spectra of 19 curcumin derivatives are presented in Table S6 and Figures S4−S41, respectively. In the $^{1}$H NMR spectrum of curcumin derivatives, peaks with chemical shifts in the range of $\delta$ 9.06−9.98, 6.59−7.8, and 3.7−3.85 were attributed to the phenolic hydroxyl group, hydrogen on the benzene ring, and the methoxy group, respectively. In the $^{13}$C NMR spectrum of curcumin derivatives, the chemical shifts fall within the ranges of $\delta$ 103.8−159.8 and 55.8−60.8, corresponding to the benzene ring group and the methoxy group.

**3.3. Evaluation of Pancreatic Lipase Inhibitory Activity.** The inhibitory activity of the synthesized curcumin derivatives was assessed by pancreatic lipase inhibition assays in vitro and the MST test. The inhibition rates of 19 curcumin derivatives on pancreatic lipase are presented in Figure 6 and Table 1. The results from Figure 6 indicated that the inhibitory potency of curcumin derivatives C4, A1, A4, C5, B10, A14, A5, C6, D4, B2, and A10 against pancreatic lipase consistently surpasses that of curcumin. Table 1 reveals that the $IC_{50}$ of curcumin was 142.24 $\mu$M. Curcumin derivatives C4, A1, A4, C5, B10, A14, A5, C6, D4, B2, and A10 exhibited $IC_{50}$ values of 42.83, 67.82, 70.44, 81.46, 82.67, 91.61, 95.40, 98.62, 110.97, 111.66, and 113.29 $\mu$M, respectively. They demonstrated superior inhibitory efficacy compared to curcumin. Among curcumin derivatives, compound C4 exhibited the most potent inhibitory activity, with an $IC_{50}$ value of 42.83 $\mu$M. As shown in Figure S42, the positive control drug, orlistat, demonstrated the $IC_{50}$ value of 1.02 $\mu$M.


https://doi.org/10.1021/acsomega.4c03596
ACS Omega 2024, 9, 27669−27679

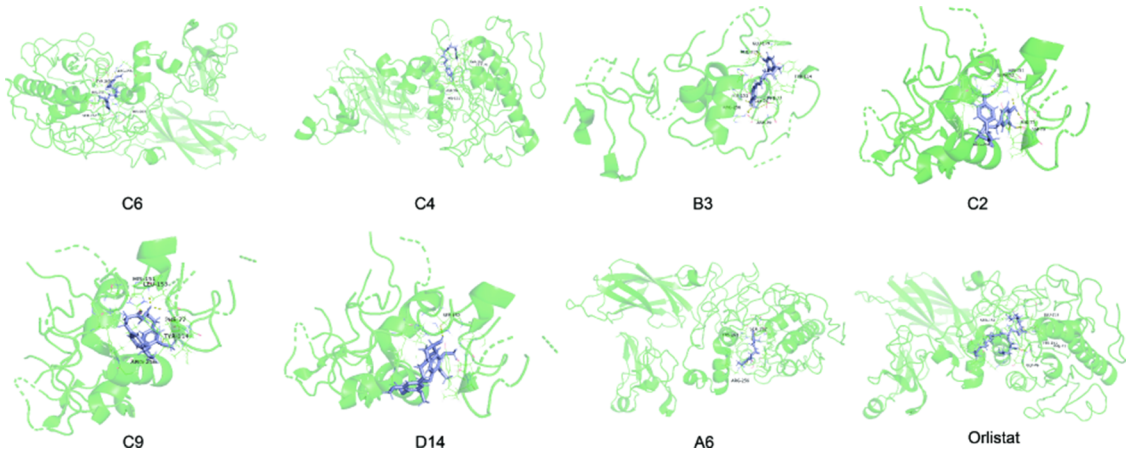


**Figure 5.** Six derivatives of curcumin (C2, C4, C6, C9, B3, and D12), along with curcumin (A6) and orlistat, were identified as potential targets for lipase activity through CADD screening.

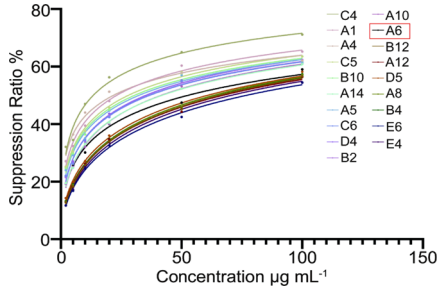


**Figure 6.** Inhibitory effect of synthetic curcumin derivatives on pancreatic lipase in vitro. The red border indicates curcumin.

**Table 1. $IC_{50}$ of Synthetic Curcumin Derivatives on Pancreatic Lipase**

| No. | $IC_{50}$ ($\mu$M) | NO. | $IC_{50}$ ($\mu$M) |
|---|---|---|---|
| orlistat | 1.02 | B2 | 111.66 |
| C4 | 42.83 | A10 | 113.29 |
| A1 | 67.82 | A6 | 142.24 |
| A4 | 70.44 | B12 | 164.45 |
| C5 | 81.46 | A12 | 168.98 |
| B10 | 82.67 | D5 | 175.02 |
| A14 | 91.61 | A8 | 187.76 |
| A5 | 95.40 | B4 | 204.32 |
| C6 | 98.62 | E6 | 235.15 |
| D4 | 110.97 | E4 | 264.63 |

C4 and C6 were two of the six curcuminoid derivatives identified through CADD screening, and they also exhibited stronger inhibitory activity in enzyme inhibition experiments, thus further conducting the MST test on C4 and C6. The affinity results of the compounds with pancreatic lipase are depicted in Figure 7. The binding constant ($K_d$) of curcumin with pancreatic lipase was 23.53 $\mu$M. For C6, the $K_d$ was 18.20 $\mu$M, and for C4, the $K_d$ was 2.91 $\mu$M. The results indicated that C4 exhibited an obviously stronger binding affinity with pancreatic lipase than curcumin. The affinity test results of orlistat with pancreatic lipase are illustrated in Figure S43, but it was incapable of fitting the affinity curve.

## 4. DISCUSSION

In this study, a set of curcumin derivatives was efficiently and swiftly screened by using CADD to identify compounds exhibiting enhanced pharmacokinetic properties and potent pancreatic lipase activity. Initially, a thorough evaluation of the pharmacokinetic properties and pancreatic lipase activity of the curcuminoid derivatives was conducted using CADD. This screening process identified 6 curcumin derivatives that exhibited superior performance in both aspects, surpassing the effectiveness of curcumin itself. Subsequently, we chemically synthesized a set of 19 curcumin derivatives as reference standards to validate the reliability of CADD. In vitro pancreatic lipase inhibition assays and MST experiments were further conducted to assess the inhibition of these derivative standards against pancreatic lipase. The curcumin derivatives C4 and C6 were ultimately selected as potential pancreatic lipase inhibitors with improved solubility and absorption characteristics. This study represented the first application of CADD to screen curcuminoids as potential pancreatic lipase inhibitors.

CADD was a technique that utilizes computer-based virtual analysis to study the activity and physicochemical properties of drugs.[34] It enabled structure-based or ligand-based drug design, encompassing methods such as molecular docking, molecular dynamics simulations, pharmacophore model screening, and molecular property prediction.[15,35] Compared with conventional methods of drug development, CADD demonstrated significant advantages in terms of shortened development cycles and cost savings. CADD played an essential role in the design of antimicrobial, antiviral, and anticancer drugs, among others, enhancing its application prospects.[15,35,36] The study utilized CADD to conduct molecular docking and property prediction evaluations of curcumin derivatives. In addition to assessing the pancreatic lipase activity and drug-likeness of curcumin derivatives, this method also simulated the dissolution, absorption, binding, and potential side effects upon oral administration of the curcumin derivatives, screening curcumin derivatives that met the desired expectations while closely mimicking the physiological conditions within the body.

The limited bioavailability of curcumin was the primary hurdle impeding its further advancement. The dissolution, absorption, and binding of curcumin derivatives within the body are closely associated with their bioavailability and distribution.[37,38] Due to the formation of hydrogen bonds between hydroxyl groups and water molecules, there was an increase in water solubility. Conversely, the $\pi-\pi$ conjugated


https://doi.org/10.1021/acsomega.4c03596
ACS Omega 2024, 9, 27669−27679

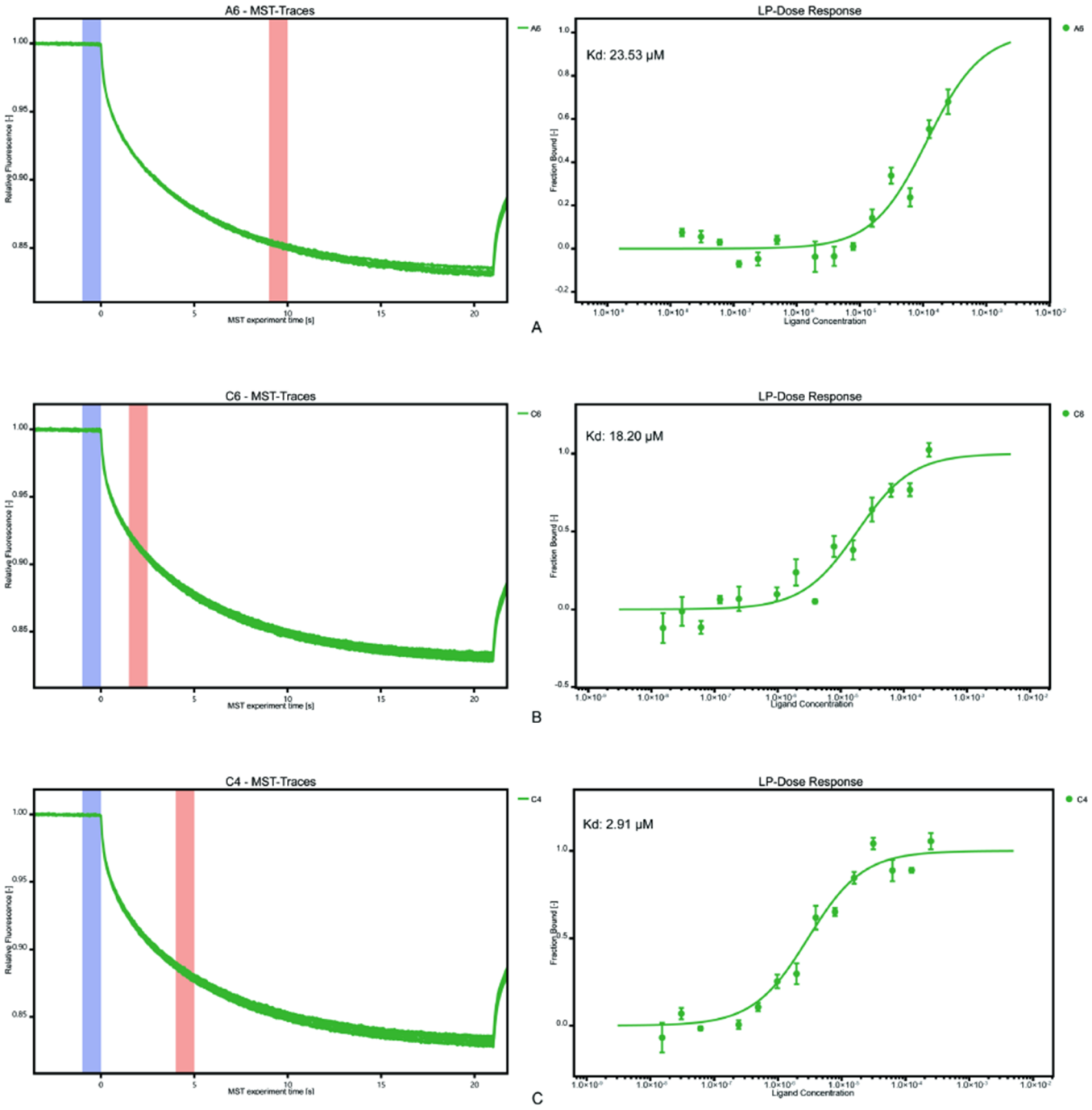


**Figure 7.** MST analysis and determination of $K_d$ for the interaction between curcumin derivatives and pancreatic lipase. A, B, and C are the binding energies of pancreatic lipase and curcumin, C6, and C4, respectively, under MST analysis.

structure and intramolecular hydrogen bonding resulted in decreased water solubility.[39−42] Among them, the C structural framework exhibited an optimal water solubility. Most curcumin derivatives exhibited low BBB permeability and high HIA. This was attributed to the acidic nature of these derivatives caused by the presence of phenolic hydroxyl groups, which affected their ability to cross the BBB. The high HIA, to some extent, indicated that structural modifications had not completely eliminated the fundamental lipophilic requirements of these derivatives.[43,44] Compounds with a higher proportion of hydroxyl groups in the benzene ring exhibited increased PPB due to the drug's ability to interact with plasma proteins through hydrogen bonding.[45] A molecule was more likely to have a lower PPB rate when it possessed fewer hydrogen bond donors or acceptors. Medications with high OB typically exhibit increased efficacy and potency, as they are more efficiently absorbed into the bloodstream, reflecting their degree of circulation within the body.[46] The OB of curcumin in this prediction model was less than 30%. Excluding derivatives within class C, those from other groups showing elevated bioavailability invariably demonstrated a diminished water solubility. Studies had indicated that this tendency might arise because fat-soluble drugs more readily penetrated capillary walls than their water-soluble counterparts when administered orally.[47] However, the bond strength between drug molecules and mucosal cell membranes was


https://doi.org/10.1021/acsomega.4c03596
ACS Omega 2024, 9, 27669−27679

excessively strong, impacting the drug's entry into the bloodstream.[48] This phenomenon restricted the speed and extent of dissolution for highly fat-soluble drugs, making it challenging to achieve optimal efficacy at a suitable dose.[49] In contrast, highly water-soluble derivatives of class C compounds exhibited elevated bioavailability compared with other compounds. This addressed the dissolution rate limitation observed in fat-soluble drugs and made them suitable candidates for drug development with enhanced bioavailability and efficacy. In molecular docking studies, orlistat inhibited PL by binding to SER-152 of pancreatic lipase at the active site.[50] It was observed that curcumin derivatives also formed associations with SER-152, indicating their potential as pancreatic lipase inhibitors. In subsequent molecular dynamics simulations, RMSD served as a metric for assessing the stability of protein−ligand complexes, where smaller values indicated greater stability.[51] The RMSD values for C6, C4, curcumin, and orlistat all fell below 3 Å, indicating the formation of relatively stable complexes with pancreatic lipase. The RMSF delineated the impact of ligands on the stability of protein amino acid residues, with greater RMSF values correlating to heightened influence.[52] In accordance with their sequence, the impact of C6, C4, orlistat, curcumin, C2, C9, B3, and D14 on protein amino acid residues sequentially intensified. The findings indicated that curcumin derivatives C4 and C6 not only formed relatively stable complexes upon binding with pancreatic lipase but also exerted a minimal influence on protein amino acid residues. Based on the results of molecular dynamics simulations, curcumin derivatives C4 and C6 emerged as the primary targets of focus for our subsequent research endeavors.

The MST experimental outcomes stemmed from the spontaneous movement induced by infrared light exposure at various temperatures upon the fluorescence complex drawn into capillary glass.[53] Compared with conventional methods for analyzing molecular interactions, it exhibited advantages such as high sensitivity, precision, real-time monitoring capability, and wide applicability. These attributes enabled the rapid and efficient assessment of the binding affinity of curcumin derivatives for lipase. The in vitro pancreatic lipase inhibition experiments and MST validation demonstrated that C4 and C6 exhibited a greater potential as pancreatic lipase inhibitors compared to curcumin, which aligned with the results obtained from CADD screening. This could be attributed to the positive correlation between the $IC_{50}$ of curcumin and its lipophilicity, where lower lipophilicity resulted in enhanced inhibitory potency.[54] The position and number of phenolic hydroxyl and methoxy groups in the phenyl ring significantly influenced the inhibitory activity of curcumin derivatives on pancreatic lipase.[30] Furthermore, additional literature studies have corroborated the superior performance of curcumin derivatives possessing these attributes in terms of absorption and activity. The removal of the methoxy group on the phenyl ring of curcumin had been demonstrated to enhance its anti-inflammatory and anticancer effects, simultaneously leading to an improvement in its water solubility.[20,55] The C6 possessing a tetracyclic framework had been proven to possess stronger antioxidant properties compared to curcumin, while also exhibiting higher bioavailability and stability.[56−58] During our previous research, we discovered that C4 was a naturally occurring derivative of curcumin found in turmeric.[32] Although there was limited existing literature concerning C4, it demonstrated superior pharmacokinetic properties and pancreatic lipase inhibitory activity compared to those of C6. The potential of C4 to overcome the undesirable properties of curcumin has heightened expectations and enthusiasm for its further development as a derivative. It was noteworthy that in the MST experiments orlistat did not successfully fit the affinity curve with pancreatic lipase. Orlistat formed a covalent bond with pancreatic lipase, impeding access of the substrate to the active site, thereby eliciting inhibitory effects. The product formed after covalent binding could not dissociate back to its unbound state; hence, orlistat could not fit the affinity curve.[59]

The study successfully employed CADD to screen and identify curcumin derivatives with potentially superior pharmacokinetic properties and enhanced pancreatic lipase inhibitory activity. This not only effectively screened curcumin derivatives capable of serving as potential pancreatic lipase inhibitors but also held significant guiding value for related studies on structural modifications of other lead compounds.[60,61] There are still some limitations that should be considered. Relying solely on CADD analysis, the screened curcumin derivatives might manifest false-positive outcomes. These compounds exhibited diverse pharmacological activities, yet their low selectivity could predispose to potential toxic side effects.[62] Hence, post-CADD, pharmacological experiments were imperative to verify the credibility of the screening results. This also constituted the primary reason for conducting subsequent in vitro pancreatic lipase assays and MST experiments. Besides, the absence of in vivo pharmacokinetic and pharmacological experiments to directly ascertain the bioavailability and activity of curcumin derivatives posed a concern that would be addressed in our subsequent research. However, based on the literature reports,[63−65] when combined with in vitro enzyme inhibition experiments and MST validation of the CADD screening results, this screening strategy had demonstrated a certain degree of efficient and reliable characteristics.

## 5. CONCLUSIONS

This study utilized CADD to perform a virtual analysis on curcumin derivatives, encompassing pharmacokinetic properties and pancreatic lipase activity. The analysis of pharmacokinetic properties involved the evaluation of curcumin derivatives' drug-likeness, LogS, HIA, BBB, PPB, H-HT, and OB using a pharmacological database of ADMET. These properties were intimately connected to the oral absorption of drugs into the body. Subsequently, molecular docking was employed to assess the inhibitory potency of curcumin derivatives against pancreatic lipase. By using the dual screening approach, 6 curcumin derivatives were identified, demonstrating superior properties in both pharmacokinetic evaluations and inhibitory activity against pancreatic lipase compared to curcumin. To further validate the reliability of CADD, a total of 19 curcumin derivative reference compounds were synthesized by considering a combination of five scaffolds and various substituents. Subsequently, the inhibitory activity and binding affinity of the 19 curcumin derivatives against pancreatic lipase were evaluated using in vitro enzyme inhibition assays and MST experiments. The results of the activity experiments were consistent with the predictions made during CADD screening. This not only confirmed the effectiveness of the strategy but also identified curcumin derivatives C4 and C6 as potential pancreatic lipase inhibitors.


https://doi.org/10.1021/acsomega.4c03596
ACS Omega 2024, 9, 27669−27679

This analytical approach aimed to provide valuable insights for screening and analyzing other compounds.

## ■ ASSOCIATED CONTENT

### Supporting Information

The Supporting Information is available free of charge at https://pubs.acs.org/doi/10.1021/acsomega.4c03596.

Name of curcumin derivatives used for CADD analysis; analysis data of curcumin derivatives using computer-aided drug design; NMR spectral data of 19 curcumin derivatives; process diagram for the synthesis of curcumin derivatives; ligand interaction diagram of C6, C4, B3, C2, C9, D14, A6, and orlistat; molecular dynamics simulations of C6, C4, B3, C2, C9, D14, A6, and orlistat; NMR spectra of 19 curcumin derivatives; orlistat's $IC_{50}$ against pancreatic lipase; MST experimental results of orlistat; and comprehensive synthetic protocols of the curcumin derivatives (PDF)

## ■ AUTHOR INFORMATION


### Corresponding Authors

**Yinping Tang** − *School of Pharmacy, Hubei University of Chinese Medicine, 430065 Wuhan, Hubei, China*; Email: yptang@hbucm.edu.cn

**Shuna Jin** − *Hubei Shizhen Laboratory, 430065 Wuhan, Hubei, China; School of Basic Medical Sciences, Hubei University of Chinese Medicine, 430065 Wuhan, Hubei, China*; orcid.org/0000-0001-7760-2382; Email: jinshuna2021@hbucm.edu.cn

### Authors

**Yuxuan Jing** − *School of Pharmacy, Hubei University of Chinese Medicine, 430065 Wuhan, Hubei, China*

**Laichun Luo** − *School of Pharmacy, Hubei University of Chinese Medicine, 430065 Wuhan, Hubei, China*

**Zhaoxiang Zeng** − *School of Pharmacy, Hubei University of Chinese Medicine, 430065 Wuhan, Hubei, China*

**Xueyan Zhao** − *School of Pharmacy, Hubei University of Chinese Medicine, 430065 Wuhan, Hubei, China*

**Rongzeng Huang** − *School of Pharmacy, Hubei University of Chinese Medicine, 430065 Wuhan, Hubei, China*

**Chengwu Song** − *School of Pharmacy, Hubei University of Chinese Medicine, 430065 Wuhan, Hubei, China; Center of Traditional Chinese Medicine Modernization for Liver Diseases, 430065 Wuhan, Hubei, China; Hubei Shizhen Laboratory, 430065 Wuhan, Hubei, China*

**Guiying Chen** − *Wuhan Hongren Biopharmaceutical Inc, 430065 Wuhan, Hubei, China*

**Sha Wei** − *School of Basic Medical Sciences, Hubei University of Chinese Medicine, 430065 Wuhan, Hubei, China*

**Haijun Yang** − *School of Basic Medical Sciences, Hubei University of Chinese Medicine, 430065 Wuhan, Hubei, China*

Complete contact information is available at: https://pubs.acs.org/10.1021/acsomega.4c03596

### Author Contributions

#Y.J., L.L., and Z.Z. contributed equally to the work.


### Notes

The authors declare no competing financial interest.

## ■ ACKNOWLEDGMENTS

This work was supported by the grants of the Natural Science Foundation of Hubei Province (No. 2022CFB486) and Science Foundation of the Department of Education of Hubei Province (No. Q20212010) and the project of the Hubei University of Chinese Medicine (No. 2022ZZXT003).

## ■ REFERENCES


(1) Singh, K.; Srichairatanakool, S.; Chewonarin, T.; Prommaban, A.; Samakradhamrongthai, R. S.; Brennan, M. A.; Brennan, C. S.; Utama-ang, N. Impact of Green Extraction on Curcuminoid Content, Antioxidant Activities and Anti-Cancer Efficiency (In Vitro) from Turmeric Rhizomes (Curcuma longa L.). *Foods* **2022**, *11*, 3633.

(2) Sharifi-Rad, J.; Rayess, Y. E.; Rizk, A. A.; Sadaka, C.; Zgheib, R.; Zam, W.; Sestito, S.; Rapposelli, S.; Neffe-Skocinska, K.; Zielinska, D.; et al. Turmeric and Its Major Compound Curcumin on Health: Bioactive Effects and Safety Profiles for Food, Pharmaceutical Biotechnological and Medicinal Applications. *Front Pharmacol* **2020**, *11*, No. 01021.

(3) Canfran-Duque, A.; Pastor, O.; Reina, M.; Lerma, M.; Cruz-Jentoft, A. J.; Lasuncion, M. A.; Busto, R. Curcumin Mitigates the Intracellular Lipid Deposit Induced by Antipsychotics In Vitro. *PLoS One* **2015**, *10*, No. e0141829.

(4) Xu, C.; Yin, L.; Teng, Z.; Zhou, X.; Li, W.; Lai, Q.; Peng, C.; Zhang, C.; Lou, J.; Zhou, X. Prevention of Obesity Related Diseases through Laminarin-induced targeted delivery of Bindarit. *Theranostics* **2020**, *10*, 9544−9560.

(5) Xie, Z.; Shen, G.; Wang, Y.; Wu, C. Curcumin supplementation regulates lipid metabolism in broiler chickens. *Poult Sci.* **2019**, *98*, 422−429.

(6) Ding, T.; Li, T.; Wang, Z.; Li, J. Curcumin liposomes interfere with quorum sensing system of Aeromonas sobria and in silico analysis. *Sci. Rep* **2017**, *7*, 8612.

(7) Rashwan, A. K.; Karim, N.; Xu, Y.; Hanafy, N. A. N.; Li, B.; Mehanni, A. E.; Taha, E. M.; Chen, W. An updated and comprehensive review on the potential health effects of curcumin-encapsulated micro/nanoparticles. *Crit. Rev. Food Sci. Nutr.* **2023**, *63*, 9731.

(8) Chen, X.; Pan, S.; Li, F.; Xu, X.; Xing, H. Plant-Derived Bioactive Compounds and Potential Health Benefits: Involvement of the Gut Microbiota and Its Metabolic Activity. *Biomolecules* **2022**, *12*, 1871−1871.

(9) Moetlediwa, M. T.; Ramashia, R.; Pheiffer, C.; Titinchi, S. J. J.; Mazibuko-Mbeje, S. E.; Jack, B. U. Therapeutic Effects of Curcumin Derivatives against Obesity and Associated Metabolic Complications: A Review of In Vitro and In Vivo Studies. *Int. J. Mol. Sci.* **2023**, *24*, 14366.

(10) Servida, S.; Panzeri, E.; Tomaino, L.; Marfia, G.; Garzia, E.; Ciniglio Appiani, G.; Moroncini, G.; De Gennaro Colonna, V.; La Vecchia, C.; Vigna, L. Overview of Curcumin and Piperine Effects on Glucose Metabolism: The Case of an Insulinoma Patient's Loss of Consciousness. *Int. J. Mol. Sci.* **2023**, *24*, 6621.

(11) Lau, A.; So, H.-C. Turning genome-wide association study findings into opportunities for drug repositioning. *Comput. Struct Biotechnol J.* **2020**, *18*, 1639−1650.

(12) Nocentini, A.; Capasso, C.; Supuran, C. T. Carbonic Anhydrase Inhibitors as Novel Antibacterials in the Era of Antibiotic Resistance: Where Are We Now? *J. Antibiot.* **2023**, *12*, 142.

(13) Kang, L.; Wang, D.; Shen, T.; Liu, X.; Dai, B.; Zhou, D.; Shen, H.; Gong, J.; Li, G.; Hu, Y.; et al. PDIA4 confers resistance to ferroptosis via induction of ATF4/SLC7A11 in renal cell carcinoma. *CELL DEATH DIS* **2023**, *14*, 193−193.

(14) Oselusi, S. O.; Dube, P.; Odugbemi, A. I.; Akinyede, K. A.; Ilori, T. L.; Egieyeh, E.; Sibuyi, N. R.; Meyer, M.; Madiehe, A. M.; Wyckoff, G. J.; et al. The role and potential of computer-aided drug discovery strategies in the discovery of novel antimicrobials. *Comput. Biol. Med.* **2024**, *169*, No. 107927.

(15) Han, D.; Lu, J.; Fan, B.; Lu, W.; Xue, Y.; Wang, M.; Liu, T.; Cui, S.; Gao, Q.; Duan, Y.; et al. Lysine-Specific Demethylase 1 Inhibitors: A Comprehensive Review Utilizing Computer-Aided Drug Design Technologies. *Molecules* **2024**, *29*, 550.
(16) Schuler, J.; Hudson, M. L.; Schwartz, D.; Samudrala, R. A Systematic Review of Computational Drug Discovery, Development, and Repurposing for Ebola Virus Disease Treatment. *Molecules* **2017**, *22*, 1777−1777.
(17) Wienken, C. J.; Baaske, P.; Rothbauer, U.; Braun, D.; Duhr, S. Protein-binding assays in biological liquids using microscale thermophoresis. *Nat. Commun.* **2010**, *1*, 100.
(18) Xiang, Y. C.; Peng, P.; Liu, X. W.; Jin, X.; Shen, J.; Zhang, T.; Zhang, L.; Wan, F.; Ren, Y. L.; Yu, Q. Q.; et al. Paris saponin VII, a Hippo pathway activator, induces autophagy and exhibits therapeutic potential against human breast cancer cells. *Acta Pharmacol Sin* **2022**, *43*, 1568−1580.
(19) Zhao, C.; Liu, Z.; Liang, G. Promising curcumin-based drug design: mono-carbonyl analogues of curcumin (MACs). *Curr. Pharm. Des.* **2013**, *19*, 2114−2135.
(20) Noureddin, S. A.; El-Shishtawy, R. M.; Al-Footy, K. O. Curcumin analogues and their hybrid molecules as multifunctional drugs. *Eur. J. Med. Chem.* **2019**, *182*, No. 111631.
(21) Chieko, K.; Hiroyuki, Y.; Atsuko, S.; Hiroshi, N.; Hisatsugu, O.; Chikashi, I.; Yoshiharu, I.; Hiroyuki, S. Synthesis of 86 species of 1,5-diaryl-3-oxo-1,4-pentadienes analogs of curcumin can yield a good lead in vivo. *BMC Pharmacol.* **2011**, *11*, 4.
(22) Dempe, J. S.; Scheerle, R. K.; Pfeiffer, E.; Metzler, M. Metabolism and permeability of curcumin in cultured Caco-2 cells. *Mol. Nutr Food Res.* **2013**, *57*, 1543−1549.
(23) Gagandeep; Singh, M.; Kidawi, S.; Das, U. S.; Velpandian, T.; Singh, R.; Rawat, D. S. Monocarbonyl curcuminoids as antituberculosis agents with their moderate in-vitro metabolic stability on human liver microsomes. *J. Biochem Mol. Toxicol* **2021**, *35*, 1−10.
(24) Shen, L.; Liu, C. C.; An, C. Y.; Ji, H. F. How does curcumin work with poor bioavailability? Clues from experimental and theoretical studies. *Sci. Rep* **2016**, *6*, 20872.
(25) Abbasi, M. A.; Raza, H.; Rehman, Aziz Ur; Siddiqui, S. Z.; Shah, S. A. A.; Hassan, M.; Seo, S.-Y Synthesis of novel N-(1,3-thiazol-2-yl)benzamide clubbed oxadiazole scaffolds: Urease inhibition, Lipinski rule and molecular docking analyses. *Bioorg. Chem.* **2018**, *83*, 63−75.
(26) Lipinski, C. A. Rule of five in 2015 and beyond: Target and ligand structural limitations, ligand chemistry structure and drug discovery project decisions. *Adv. Drug Delivery Rev.* **2016**, *101*, 34−41.
(27) Li, M.; Chen, H.; Zhang, H.; Zeng, M.; Chen, B.; Guan, L. Prediction of the Aqueous Solubility of Compounds Based on Light Gradient Boosting Machines with Molecular Fingerprints and the Cuckoo Search Algorithm. *ACS Omega* **2022**, *7*, 42027−42035.
(28) Mazumder, A.; Neamati, N.; Sunder, S.; Schulz, J.; Pertz, H.; Eich, E.; Pommier, Y. Curcumin analogs with altered potencies against HIV-1 integrase as probes for biochemical mechanisms of drug action. *J. Med. Chem.* **1997**, *40*, 3057−3063.
(29) Zhao, C.; Zhang, Y.; Zou, P.; Wang, J.; He, W.; Shi, D.; Li, H.; Liang, G.; Yang, S. Synthesis and biological evaluation of a novel class of curcumin analogs as anti-inflammatory agents for prevention and treatment of sepsis in mouse model. *Drug Des Devel Ther* **2015**, *9*, 1663−1678.
(30) Cardullo, N.; Muccilli, V.; Pulvirenti, L.; Tringali, C. Natural Isoflavones and Semisynthetic Derivatives as Pancreatic Lipase Inhibitors. *J. Nat. Prod* **2021**, *84*, 654−665.
(31) Sridhar, S. N. C.; Palawat, S.; Paul, A. T. Design, synthesis, biological evaluation and molecular modelling studies of indole glyoxylamides as a new class of potential pancreatic lipase inhibitors. *Bioorg Chem.* **2019**, *85*, 373−381.
(32) Xiang, X.; Song, C.; Shi, Q.; Tian, J.; Chen, C.; Huang, J.; She, B.; Zhao, X.; Huang, R.; Jin, S. A novel predict-verify strategy for targeted metabolomics: Comparison of the curcuminoids between crude and fermented turmeric. *Food Chem.* **2020**, *331*, No. 127281.
(33) Jin, S.; Song, C.; Jia, S.; Li, S.; Zhang, Y.; Chen, C.; Feng, Y.; Xu, Y.; Xiong, C.; Xiang, Y.; et al. An integrated strategy for establishment of curcuminoid profile in turmeric using two LC−MS/MS platforms. *J. Pharm. Biomed Anal* **2017**, *132*, 93−102.
(34) Zhang, X.; Chen, H.; Lin, H.; Wen, R.; Yang, F. High-Throughput Screening and Molecular Dynamics Simulation of Natural Products for the Identification of Anticancer Agents against MCM7 Protein. *Appl. Bionics. Biomech.* **2022**, *2022*, No. 8308192.
(35) Dai, R.; Gao, H.; Su, R. Computer-aided drug design for virtual-screening and active-predicting of main protease (Mpro) inhibitors against SARS-CoV-2. *Front Pharmacol* **2023**, *14*, 1288363−1288363.
(36) Rashdan, H. R. M.; Abdelmonsef, A. H.; Abou-Krisha, M. M.; Yousef, T. A. Synthesis, Identification, Computer-Aided Docking Studies, and ADMET Prediction of Novel Benzimidazo-1,2,3-triazole Based Molecules as Potential Antimicrobial Agents. *Molecules* **2021**, *26*, 7119−7119.
(37) Bharti, G.; Varsha, M.; Sankalp, G.; Munira, M.; Abdelwahab, O. Cellulosic Polymers for Enhancing Drug Bioavailability in Ocular Drug Delivery Systems. *Pharmaceuticals* **2021**, *14*, 1201.
(38) Gupta, P.; Panwar, U.; Singh, S. Novel scaffolds identification against Mpro of SARS-CoV-2 using shape based screening and molecular simulation methods. *Chemical Physics Impact* **2024**, *8*, No. 100496.
(39) Martinez, J.; Ramírez, C.; Gil, J.; Quiñones, W.; Durango, D. Antifungal activity against anthracnose-causing species of homopterocarpin derivatives. *Heliyon* **2023**, *9*, No. e13082.
(40) Tachibana, Y.; Hayashi, S.; Kasuya, K.-I Biobased Poly(Schiff-Base) Composed of Bifurfural. *ACS Omega* **2018**, *3*, 5336−5345.
(41) Chaudhari, S. R.; Griffin, J. M.; Broch, K.; Lesage, A.; Lemaur, V.; Dudenko, D.; Olivier, Y.; Sirringhaus, H.; Emsley, L.; Grey, C. P. Donor−acceptor stacking arrangements in bulk and thin-film high-mobility conjugated polymers characterized using molecular modelling and MAS and surface-enhanced solid-state NMR spectroscopy. *Chem. Sci.* **2017**, *8*, 3126−3136.
(42) Liu, R.-Z.; Li, W.-J.; Zhang, J.-J.; Liu, Z.-Y.; Li, Y.; Liu, C.; Qin, S. The Inhibitory Effect of Phycocyanin Peptide on Pulmonary Fibrosis In Vitro. *Mar Drugs* **2022**, *20*, 696.
(43) Ghose, A. K.; Herbertz, T.; Hudkins, R. L.; Dorsey, B. D.; Mallamo, J.P.J.A.C.N. Knowledge-Based Central Nervous System (CNS) Lead Selection and Lead Optimization for CNS Drug Discovery. *ACS Chem. Neurosci.* **2012**, *3*, 50−68.
(44) Cawley, J. R.; Stewart, S. D.; Mochel, J. P.; Veluvolu, S.; Khanna, C.; Fenger, J. M. Pharmacokinetic Exposures Associated With Oral Administration of Sorafenib in Dogs With Spontaneous Tumors. *Front Vet Sci.* **2022**, *9*, No. 888483.
(45) Zhao, M.-L.; Liu, X.-Q.; Cao, Y.; Li, X.-F.; Li, D.-J.; Sun, X.-L.; Gu, H.-Q.; Wan, R.-X Enhancement of interaction of L-929 cells with functionalized graphene via COOH+ ion implantation vs. chemical method. *Sci. Rep* **2016**, *6*, 37112.
(46) Songvut, P.; Boonyarattanasoonthorn, T.; Nuengchamnong, N.; Junsai, T.; Kongratanapasert, T.; Supannapan, K.; Khemawoot, P. Enhancing oral bioavailability of andrographolide using solubilizing agents and bioenhancer: comparative pharmacokinetics of Andrographis paniculata formulations in beagle dogs. *Pharm. Biol.* **2024**, *62*, 183−194.
(47) Elwan, H.; Xie, C.; Miao, L. P.; Dong, X.; Zou, X. t.; Mohany, M.; Ahmed, M. M.; Al-Rejaie, S. S.; Elnesr, S. S. Methionine alleviates aflatoxinb1-induced broiler chicks embryotoxicity through inhibition of caspase-dependent apoptosis and enhancement of cellular antioxidant status. *Poultry Science* **2021**, *100*, No. 101103.
(48) Chen, Y.-C.; Li, W.-C.; Ke, P.-H.; Chen, I. C.; Yu, W.; Huang, H.-Y.; Xiong, X.-J.; Chen, J.-Y. Association between metabolic body composition status and vitamin D deficiency: A cross-sectional study. *Front Nutr* **2022**, *9*, No. 940183.
(49) Ahmed, T. A.; Alotaibi, H. A.; Alharbi, W. S.; Safo, M. K.; El-Say, K. M. Development of 3D-Printed, Liquisolid and Directly Compressed Glimepiride Tablets, Loaded with Black Seed Oil Self-Nanoemulsifying Drug Delivery System: In Vitro and In Vivo Characterization. *Pharmaceuticals* **2022**, *15*, 68−68.


https://doi.org/10.1021/acsomega.4c03596
*ACS Omega* 2024, 9, 27669−27679

(50) Almasri, I. M. Computational approaches for the discovery of natural pancreatic lipase inhibitors as antiobesity agents. *Future Med. Chem.* **2020**, *12*, 741−757.
(51) Bhardwaj, P.; Biswas, G. P.; Mahata, N.; Ghanta, S.; Bhunia, B. Exploration of binding mechanism of triclosan towards cancer markers using molecular docking and molecular dynamics. *Chemosphere* **2022**, *293*, No. 133550.
(52) Barcellos, M. P.; Santos, C. B. R.; Federico, L. B.; Almeida, P. F.; da Silva, C.; Taft, C. A. Pharmacophore and structure-based drug design, molecular dynamics and admet/tox studies to design novel potential pad4 inhibitors. *J. Biomol Struct Dyn* **2019**, *37*, 966−981.
(53) Fulvio, C.; Vincenzo, D. L.; Lucia, C.; Michelangelo, P.; A, F. L.; M, C. D.; Annalisa, D. G. An In-Silico Pipeline for Rapid Screening of DNA Aptamers against Mycotoxins: The Case-Study of Fumonisin B1, Aflatoxin B1 and Ochratoxin A. *Polymers* **2020**, *12*, 2983.
(54) Ji, Z.; Sang, J.; Wang, H.; Xia, M.; Hao, T.; Chen, L.; Lu, H.; Wang, S.; Yao, M.; Li, L.; et al. Demethoxylation of curcumin enhances its inhibition on human and rat 17beta-hydroxysteroid dehydrogenase 3: QSAR structure-activity relationship and in silico docking analysis. *Food Chem. Toxicol.* **2024**, *186*, No. 114489.
(55) Nagaraju, G. P.; Benton, L.; Bethi, S. R.; Shoji, M.; El-Rayes, B. F. Curcumin analogs: Their roles in pancreatic cancer growth and metastasis. *Int. J. Cancer* **2019**, *145*, 10−19.
(56) Lawrence, H.; Gordon, B.; Muhammed, M.; Brigitta, V.; Kresimir, P.; Dharmendr, M. Infusion pharmacokinetics of Lipocurc (liposomal curcumin) and its metabolite tetrahydrocurcumin in Beagle dogs. *Anticancer Res.* **2012**, *32*, 4365−4370.
(57) Panda, S. K.; Nirvanashetty, S.; Missamma, M.; Jackson-Michel, S. The enhanced bioavailability of free curcumin and bioactive-metabolite tetrahydrocurcumin from a dispersible, oleoresin-based turmeric formulation. *Medicine* **2021**, *100*, No. e26601.
(58) Girst, G.; Otvos, S. B.; Fulop, F.; Balogh, G. T.; Hunyadi, A. Pharmacokinetics-Driven Evaluation of the Antioxidant Activity of Curcuminoids and Their Major Reduced Metabolites-A Medicinal Chemistry Approach. *Molecules* **2021**, *26*, 3542−3542.
(59) Banni, G. A. D.; Nasreddine, R.; Fayad, S.; Colas, C.; Marchal, A.; Nehmé, R. Investigation of lipase-ligand interactions in porcine pancreatic extracts by microscale thermophoresis. *Anal. Bioanal. Chem.* **2021**, *413*, 3667−3681.
(60) Yang, L.; Jianhong, G.; Rongqi, W.; Xiaocong, Y.; Zhixiong, X.; Yang, C. DrugDevCovid19: An Atlas of Anti-COVID-19 Compounds Derived by Computer-Aided Drug Design. *Molecules* **2022**, *27*, 683.
(61) Gaudêncio, S. P.; Pereira, F. Predicting Antifouling Activity and Acetylcholinesterase Inhibition of Marine-Derived Compounds Using a Computer-Aided Drug Design Approach. *Mar. Drugs* **2022**, *20*, 129.
(62) Barakat, A.; Munro, G.; Heegaard, A. M. Finding new analgesics: Computational pharmacology faces drug discovery challenges. %J. *Biochemical pharmacology.* **2024**, *222*, No. 116091.
(63) Sun, C.; He, Y.; Wang, G.; Zhang, G.; Zhang, Y.; Shen, H.; Hu, L.; Sun, Y.; Jiang, B.; Wang, X.; et al. Design, Synthesis, and Antitumor Activity Evaluation of Novel VISTA Small Molecule Inhibitors. *J. Med. Chem.* **2024**, *67*, 3590−3605.
(64) Yuan, C.; Tian, J.; Zhou, Q.; Xin, H.; Liu, Y.; Deng, T.; Zeng, W.; Sun, Z.; Xue, W. Myricetin derivatives containing the benzoxazinone moiety discovered as potential anti-tobacco mosaic virus agents. *Fitoterapia* **2024**, *173*, No. 105812.
(65) Fassi, E. M. A.; Manenti, M.; Citarella, A.; Dei Cas, M.; Casati, S.; Micale, N.; Schirmeister, T.; Roda, G.; Silvani, A.; Grazioso, G. Computational Design, Synthesis, and Biophysical Evaluation of *β*-Amido Boronic Acids as SARS-CoV-2 M(pro). *Inhibitors. Molecules* **2023**, *28*, 2356−2356.


https://doi.org/10.1021/acsomega.4c03596
*ACS Omega* 2024, 9, 27669−27679